

NUMERICAL SCHEMES FOR A FULLY NONLINEAR COAGULATION-FRAGMENTATION MODEL COMING FROM WAVE KINETIC THEORY

ARIJIT DAS AND MINH-BINH TRAN

ABSTRACT. This article introduces a novel numerical approach, based on Finite Volume Techniques, for studying fully nonlinear coagulation-fragmentation models, where both the coagulation and fragmentation components of the collision operator are nonlinear. The models come from 3-wave kinetic equations, a pivotal framework in wave turbulence theory. Despite the importance of wave turbulence theory in physics and mechanics, there have been very few numerical schemes for 3-wave kinetic equations, in which no ad-hoc additional assumptions are imposed on the evolution of the solutions, and the current manuscript provides one of the first of such schemes. To the best of our knowledge, this also is the first numerical scheme capable of accurately capturing the long-term asymptotic behavior of solutions to a fully nonlinear coagulation-fragmentation model that includes both forward and backward energy cascades. The scheme is implemented on some test problems, demonstrating strong alignment with theoretical predictions of energy cascade rates. We further introduce a weighted Finite Volume variant to ensure energy conservation across varying degrees of kernel homogeneity. Convergence and first-order consistency are established through theoretical analysis and verified by experimental convergence orders in test cases.

1. INTRODUCTION

Over the past six decades, the theory of wave turbulence has been shown to play important roles in a vast range of physical and mechanical examples including inertial waves due to rotation, Alfvén wave turbulence in the solar wind, waves in plasmas of fusion devices, and many others. Building on Peierls' foundational work [1], the theory's modern development has been driven by contributions from Benney and Saffman [2], Zakharov and Falkovich [3], Benney and Newell [4] and especially the groundbreaking Nobel laureate work of Hasselmann [5, 6]. These efforts culminated in the formulation of 3-wave and 4-wave kinetic equations, which describe the energy distribution among weakly interacting waves. The general form of 3-wave kinetic equations reads

$$(1.1) \quad \partial_t f(t, p) = \iint_{\mathbb{R}^{2d}} \left[R_{p, p_1, p_2}[f] - R_{p_1, p, p_2}[f] - R_{p_2, p, p_1}[f] \right] dp_1 dp_2, \quad f(0, p) = f_0(p),$$

where $f(t, p)$ is the wave density at wavenumber $p \in \mathbb{R}^d$, $d \geq 2$ and $f_0(p)$ is the initial condition. Moreover,

$$(1.2) \quad R_{p, p_1, p_2}[f] := |V_{p, p_1, p_2}|^2 \delta(p - p_1 - p_2) \delta(\Omega - \Omega_1 - \Omega_2) (f_1 f_2 - f f_1 - f f_2),$$

2020 *Mathematics Subject Classification.* 65M08, 45K05, 76F55.

Key words and phrases. Wave turbulence; 3-wave kinetic; Coagulation-fragmentation equation; Finite volume method; energy decay, Numerical analysis.

with the short-hand notations $f = f(t, p)$, $\Omega = \Omega(p)$ and $f_j = f(t, p_j)$, $\Omega_j = \Omega(p_j)$, for $p, p_j, j \in \{1, 2\}$. The quantity $\Omega(p)$ is the dispersion relation of the waves. For a deeper physical understanding, we refer to the comprehensive works in [7, 8, 9].

In a related context, coagulation and fragmentation kinetic equations arise in several physical and mechanical contexts: the formation of aerosols, polymers, celestial bodies on astronomical scales or colloidal aggregates (see [10, 11, 12, 13, 14, 15, 16, 17, 18, 19, 20, 21] and the references therein). Coagulation-fragmentation kinetic equation describes the behavior of particles that coagulate or fragment due to the mutual interactions or some external force. The primary quantity of interest in this field is the particle number density function, typically denoted $n_\omega(t)$, representing the density of clusters of size ω at time t . For pure coagulation, the Smoluchowski coagulation equation serves as the classical model of particulate processes. Coagulation-fragmentation kinetics plays a crucial role in wave turbulence theory. Despite the difference in focus, there is a conceptual analogy between coagulation-fragmentation kinetics and 3-wave kinetic models: the transfer of energy between scales in wave turbulence is analogous to the transfer of mass between clusters in coagulation processes. This observation offers a quantitative bridge between the two fields. Building on this analogy, Connaughton proposed an approximation of the 3-wave kinetic equations (1.1)-(1.2) using a nonlinear coagulation-fragmentation model [22, 23, 24]. In contrast to standard models, Connaughton's formulation incorporates nonlinearities in both the coagulation and fragmentation terms of the collision operator. Connaughton's model is given in [22, 23, 24]

$$(1.3) \quad \frac{\partial N_\omega}{\partial t} = \mathcal{Q}[N_\omega](t), \quad \omega \in \mathbb{R}_+, \quad N_\omega(0) = N_\omega^{in}.$$

The operator $\mathcal{Q}[N_\omega](t)$ can be expressed as

$$(1.4) \quad \mathcal{Q}[N_\omega](t) = S_1[N_\omega] - S_2[N_\omega] - S_3[N_\omega],$$

and

$$\begin{aligned} S_1[N_\omega] &= \int_0^\omega K_1(\omega - \mu, \mu) N_{\omega-\mu} N_\mu d\mu - \int_\omega^\infty K_1(\mu - \omega, \omega) N_{\mu-\omega} N_\omega d\mu \\ &\quad - \int_0^\infty K_1(\omega, \mu) N_\omega N_\mu d\mu \\ &= \int_0^\omega K_1(\omega - \mu, \mu) N_{\omega-\mu} N_\mu d\mu - 2 \int_0^\infty K_1(\omega, \mu) N_\omega N_\mu d\mu, \\ S_2[N_\omega] &= - \int_0^\omega K_2(\mu, \omega - \mu) N_\omega N_\mu d\mu + \int_\omega^\infty K_2(\omega, \mu - \omega) N_{\mu-\omega} N_\omega d\mu \\ &\quad + \int_0^\infty K_2(\omega, \mu) N_\omega N_{\omega+\mu} d\mu, \\ S_3[N_\omega] &= - \int_0^\omega K_3(\mu, \omega - \mu) N_\omega N_{\omega-\mu} d\mu + \int_\omega^\infty K_3(\omega, \mu - \omega) N_\omega N_\mu d\mu \\ &\quad + \int_0^\infty K_3(\omega, \mu) N_\mu N_{\omega+\mu} d\mu. \end{aligned}$$

The wave frequency spectrum N_ω is defined such that $\int_{\omega_1}^{\omega_2} N_\omega d\omega$ represents the total wave action in the frequency band $[\omega_1, \omega_2]$. To analyze solutions to the nonlinear coagulation-fragmentation model (1.3), we define the p -th moment as:

$$M_p(t) = \int_0^\infty \omega^p N_\omega(t) d\omega, \quad \text{for all } p \geq 0.$$

In this regard, the total number of wave N and total wave energy E can be obtained from the zeroth and first moments, respectively. Specifically, we have:

$$N = \int_0^\infty N_\omega d\omega, \quad E = \int_0^\infty \omega N_\omega d\omega.$$

Also, the nonnegative homogeneous functions $K_i(\omega, \mu)$ ($i = 1, 2, 3$) represent the wave interaction kernels, exhibiting a degree of homogeneity $(2\beta - \alpha)/\alpha$. Here, α, β be the degree of homogeneity of wave dispersion relation and wave-wave interaction coefficient, respectively. Among these kernels, K_1 facilitates the forward transfer of energy, while K_2 and K_3 are associated with the back-scattering of energy.

Since developing numerical schemes for 3-wave kinetic equations is highly important to understand the time evolution of the solutions, in [22, 23, 24], the authors constructed several numerical schemes for (1.3) by adopting a self-similar hypothesis known as dynamical scaling, where the kernels are chosen as

$$(1.5) \quad K_1(\omega, \mu) = K_2(\omega, \mu) = K_3(\omega, \mu) = (\omega\mu)^{\frac{\lambda}{2}}.$$

Under this assumption, the solution N_ω is hypothesized to evolve toward a scaling (self similar) form $N_\omega \sim S(t)^a F\left(\frac{\omega}{S(t)}\right)$. Here \sim denote the scaling limit: $S(t) \rightarrow 0$ as $\omega \rightarrow \infty$. For $x = \omega/S(t)$ the total energy corresponding to the self similar profile F is given by

$$(1.6) \quad E = \int_0^\infty \omega S(t) F\left(\frac{\omega}{S(t)}\right) d\omega = \int_0^\infty x S(t)^{a+2} F(x) dx = S(t)^{a+2} \int_0^\infty x F(x) dx \sim \mathcal{O}(S(t)^{a+2}),$$

which grow with the rate $\mathcal{O}(S(t)^{a+2})$. Now using this ansatz into the equation (1.3) with the choice (1.5), one can obtain the system

$$(1.7) \quad \frac{dS(t)}{dt} = S(t)^\xi, \quad \text{with } \xi = \lambda + a + 2, \quad aF(x) + x\dot{F}(x) = \mathcal{Q}[F](x).$$

It can be observed that the energy is conserved only when $a = -2$. Under this condition, the authors in [22, 23, 24] deduced that under the additional assumption that the self-similar profile exhibits power-law behavior, i.e. $F(x) \sim Ax^{-m}$ as $x \sim 0$ then $m = \lambda + 1$. Note that this condition is also necessary to ensure the convergence of the integral

$$(1.8) \quad \int_0^\infty x F(x) dx,$$

they consider the range of the λ is $[0, 1]$. However, there is a problem for the finite capacity case as the integral (1.8) diverges for $\lambda > 1$. In [22, 23, 24], the authors consider $\lambda \in [0, 2]$ under another assumption that the total energy of the solution to equation (1.3) is assumed to grow linearly with time, rather than maintaining constant initial energy $\int_0^\infty \omega N_\omega d\omega = Jt$. This leads

to the ODE $\frac{dS}{dt} = \frac{J}{(a+2) \int_0^\infty xF(x)dx} S(t)^{-a-1}$. By comparing this with the equation (1.7), one obtains $a = -\frac{\lambda+3}{2}$, the KZ-value. So, in this case the self-similar profile $F \sim x^{-\frac{\lambda+3}{2}}$ makes the integral (1.8) divergent for the finite capacity case. Consequently, further assumptions need to be imposed on the evolution of the solution N_ω itself.

Therefore, the primary goal of this article is to develop a numerical scheme for the fully nonlinear coagulation-fragmentation model (1.3) that, unlike the approaches in [22, 23, 24], does not impose additional ad-hoc assumptions on the evolution of solutions. This scheme is designed for several choices of kernels:

$$K_1(\omega, \mu) = (\omega\mu)^\theta, \quad K_2(\omega, \mu) = (\omega\mu)^\gamma, \quad K_3(\omega, \mu) = (\omega\mu)^\delta.$$

It is worth noting that in [25] and [26], the authors proposed numerical schemes for a *specific 3-wave kinetic equation*, derived from the theory of capillary and acoustic waves. In these works, the authors formulated a conservative representation of the kinetic model and proposed a numerical scheme demonstrating good agreement with theoretical decay phenomena. However, these schemes relied on the *exact formulation* (1.1)-(1.2) of a *specific 3-wave kinetic equation*, rather than the *approximation of all 3-wave kinetic equations* by a fully nonlinear coagulation-fragmentation model. Since Connaughton's approximation represents one of the first fully nonlinear models in the literature, it is important to numerically investigate the behavior of its solutions. *The numerical schemes introduced in the current work, together with those proposed in [25] and [26], are among the first numerical schemes for 3-wave kinetic equations, in which no ad-hoc additional assumptions need to be imposed on solutions themselves. Even though there have been quite a lot of numerical works on coagulation-fragmentation models (see for instance [27]), to our best knowledge, the current manuscript is the first work that conducts numerical studies for a fully nonlinear coagulation-fragmentation model, where both coagulation-fragmentation parts are nonlinear.*

Let us discuss about the works [28, 29] where numerical methods have been employed to solve various types of wave turbulence kinetic equations. In [28], the author computed the self-similar profile of the Alfvén wave turbulence kinetic equation, illustrating different finite capacities. The work by [29] presents a numerical technique based on Chebyshev approximation to solve the self-similar profile before the first blow-up time for a 4-wave kinetic equation.

Theoretical studies of 3-wave kinetic equations span diverse contexts, such as phonon interactions in an-harmonic crystal lattices [30, 31, 32, 33], capillary waves [34, 35], beam waves [36], stratified ocean flows [32], and Bose-Einstein Condensates [37, 38, 39, 40, 41, 34, 42]. In addition, 4-wave kinetic equations have been analyzed in the pioneering work of Escobedo and Velazquez [43, 44], as well as other works [45, 46, 47, 48, 49, 50, 51, 52]. Rigorous derivations of wave kinetic equations are provided in [53, 54, 55, 56, 57, 58, 59, 60, 61, 62, 63, 64, 65, 66, 67, 68, 69, 70, 71] and the references therein.

From this discussion, it is clear that developing a numerical scheme for the fully nonlinear coagulation-fragmentation model (1.3) is a pressing and unexplored task in the literature. At the same time the numerical observation of the theoretical results for the time dependent solution also becomes necessary for both scientific understanding and application. Therefore, the primary

objective of this article is to develop a novel numerical scheme for the fully nonlinear coagulation-fragmentation model (1.3). Unlike the approach taken in [25, 26], we design our numerical scheme by discretizing the fully nonlinear coagulation-fragmentation model (1.3), rather than the conservative form of the 3-wave kinetic equations. More specifically, the primary focus of this study is on the derivation of a finite volume scheme (FVS) that allows us to investigate the behavior of the solutions to (1.3). To ensure energy conservation, particularly for wave kernels with relatively small degrees of homogeneity, we propose an alternative weighted finite volume scheme (FVS) that incorporates specific weight functions. In addition to formulating these numerical schemes, this article provides a comprehensive analysis of the convergence of the proposed scheme. We further demonstrate that the scheme is first-order consistent, which is verified through experimental order of convergence calculations across various test cases.

The remainder of this article is organized as follows: In Section 2, we formulate the finite volume scheme for the fully nonlinear coagulation-fragmentation model and introduce the newly formulated weighted FVS, proving its ability to conserve total energy. Section 3 is dedicated to a detailed convergence analysis of the proposed FVS. In Section 4, we present numerical simulations to validate the theoretical results for the fully nonlinear coagulation-fragmentation model.

Acknowledgment We would like to express our gratitude to Dr. Iulia Cristian, Dr. Steven Walton, Professor Avy Soffer and Professor Enrique Zuazua for fruitful discussions on the topics. A. D. expresses gratitude to the Chair for Dynamics, Control, Machine Learning, and Numerics in the Department of Mathematics at FAU Erlangen-Nurnberg for their hospitality, where the work was conducted. M.-B. T is funded in part by a Humboldt Fellowship, NSF CAREER DMS-2303146, and NSF Grants DMS-2204795, DMS-2305523, DMS-2306379.

2. FORMULATION OF FINITE VOLUME SCHEME

For the mathematical formulation of a numerical scheme, we need to truncate the given in a finite computational domain $\mathcal{D} = (0, R]$. Let us consider the following truncated form of the fully nonlinear coagulation-fragmentation model equation

$$(2.1) \quad \frac{\partial N_\omega}{\partial t} = S_1^{nc} [N_\omega] - S_2^c [N_\omega] - S_3^c [N_\omega], \quad \omega \in \mathbb{R}_+.$$

Here

$$\begin{aligned} S_1^{nc} [N_\omega] &= \int_0^\omega K_1(\omega - \mu, \mu) N_{\omega-\mu} N_\mu d\mu - 2 \int_0^R K_1(\omega, \mu) N_\omega N_\mu d\mu, \\ S_2^c [N_\omega] &= - \int_0^\omega K_2(\mu, \omega - \mu) N_\omega N_\mu d\mu + \int_\omega^R K_2(\omega, \mu - \omega) N_{\mu-\omega} N_\mu d\mu \\ &\quad + \int_0^{R-\omega} K_2(\omega, \mu) N_\omega N_{\omega+\mu} d\mu, \\ S_3^c [N_\omega] &= - \int_0^\omega K_3(\mu, \omega - \mu) N_\omega N_{\omega-\mu} d\mu + \int_\omega^R K_3(\omega, \mu - \omega) N_\omega N_\mu d\mu \\ &\quad + \int_0^{R-\omega} K_3(\omega, \mu) N_\mu N_{\mu+\omega} d\mu. \end{aligned}$$

For the numerical scheme, let us discretize the computational domain \mathcal{D} into I number of cells with the limits 0 to $R < \infty$. Moreover, each of the i -th sub interval for $i \in \{0, 1, 2, \dots, I\}$, is denoted by $\Lambda_i := [\omega_{i-1/2}, \omega_{i+1/2}]$ and the cell representative of the i -th cell is given by

$$\omega_{1/2} = 0, \quad \omega_{I+1/2} = R, \quad \omega_i = \frac{\omega_{i-1/2} + \omega_{i+1/2}}{2}.$$

Furthermore, introduce the bound $\Delta\omega$ and $\Delta\omega_{min}$ as follows $\Delta\omega_{min} \leq \omega_{i+1/2} - \omega_{i-1/2} := \Delta\omega_i \leq \Delta\omega$. The integration of the truncated fully nonlinear coagulation-fragmentation model over each cell gives the discretized scheme in \mathbb{R}^I as

$$(2.2) \quad \frac{d\mathbf{N}}{dt} = \mathbf{J}(\mathbf{N}) := \sum_{k=1}^5 \mathbf{Q}^k, \quad \text{with } \mathbf{N}(0) = \mathbf{N}^{in}.$$

Where $\mathbf{N}, \mathbf{N}^{in}$, and \mathbf{Q}^k for $(k = 1, 2, \dots, 5)$ are all in \mathbb{R}^I . The i -th component of these vectors are given by

$$(2.3) \quad N_i(t) = \int_{\omega_{i-1/2}}^{\omega_{i+1/2}} N_\omega(t) d\omega, \quad \text{with } N_i^{in}(t) = \int_{\omega_{i-1/2}}^{\omega_{i+1/2}} N_\omega(0) d\omega,$$

$$(2.4) \quad Q_i^1(t) = \int_{\omega_{i-1/2}}^{\omega_{i+1/2}} \int_0^\omega K_1(\omega - \mu, \mu) N_{\omega-\mu} N_\mu d\mu d\omega,$$

$$(2.5) \quad Q_i^2(t) = -2 \int_{\omega_{i-1/2}}^{\omega_{i+1/2}} \int_0^R K_1(\omega, \mu) N_\omega N_\mu d\mu,$$

$$(2.6) \quad Q_i^3(t) = \int_{\omega_{i-1/2}}^{\omega_{i+1/2}} \left[\int_\omega^R K_2(\omega, \mu - \omega) N_{\mu-\omega} N_\mu d\mu + \int_0^{R-\omega} K_3(\omega, \mu) N_\mu N_{\mu+\omega} d\mu \right] d\omega,$$

$$(2.7) \quad Q_i^4(t) = - \int_{\omega_{i-1/2}}^{\omega_{i+1/2}} \left[\int_0^\omega K_2(\mu, \omega - \mu) N_\omega N_\mu d\mu + \int_0^\omega K_3(\mu, \omega - \mu) N_\omega N_{\omega-\mu} d\mu \right] d\omega,$$

$$(2.8) \quad Q_i^5(t) = \int_{\omega_{i-1/2}}^{\omega_{i+1/2}} \left[\int_0^{R-\omega} K_2(\omega, \mu) N_\omega N_{\omega+\mu} d\mu + \int_\omega^R K_3(\omega, \mu - \omega) N_\omega N_\mu d\mu \right] d\omega.$$

Moreover, for a fully discrete formulation, the time domain need to discretized. To discretize the time variable t , we split the time interval $[0, T]$ into N subintervals $\tau_n := [t_n, t_{n+1})$, for $n \in \{0, 1, \dots, N-1\}$, with $t_n = n\Delta t$ and $N\Delta t = T$. The above discretization of volume variable x and time variable t leads to the discretize form of the collision kernel as follows; for $i, j \in \{1, \dots, I\}$

$$K_1(u, v) \approx K_1^h(u, v) = K_{i,j}^1, \quad \text{when } u \in \Lambda_i, v \in \Lambda_j,$$

$$K_2(u, v) \approx K_2^h(u, v) = K_{i,j}^2, \quad \text{when } u \in \Lambda_i, v \in \Lambda_j,$$

$$K_3(u, v) \approx K_3^h(u, v) = K_{i,j}^3, \quad \text{when } u \in \Lambda_i, v \in \Lambda_j.$$

The numerical values approximating $N_i(t)$ at time t_n is denoted by N_i^n . Therefore, the wave density function can be represented as

$$(2.9) \quad N_\omega \approx \sum_{i=1}^I N_i^n \Delta\omega_i \delta(\omega - \omega_i).$$

To formulate the numerical scheme, we also need to the following sets of indices as

$$\begin{aligned}\mathcal{I}_{j,k}^i &:= \{(j, k) \in \mathbb{N} \times \mathbb{N} : \omega_{i-1/2} \leq \omega_j + \omega_k < \omega_{i+1/2}\}, \\ \mathcal{J}_{j,k}^i &:= \{(j, k) \in \mathbb{N} \times \mathbb{N} : \omega_{i-1/2} \leq \omega_j - \omega_k < \omega_{i+1/2}\}, \\ \mathcal{K}_{j,k}^* &:= \{(j, k) \in \mathbb{N} \times \mathbb{N} : \omega_j + \omega_k > R\}.\end{aligned}$$

Using the aforementioned notation of the index sets with the approximation (2.9), the numerical *Finite Volume Scheme* (FVS) can be written as follows:

$$(2.10) \quad \begin{aligned}N_i^{n+1} = N_i^n + \Delta t^n &\left(\sum_{(j,k) \in \mathcal{I}_{j,k}^i} K_{j,k}^1 N_j^n N_k^n \frac{\Delta \omega_j \Delta \omega_k}{\Delta \omega_i} - 2 \sum_{j=1}^I K_{i,j}^1 N_i^n N_j^n \Delta \omega_j \right. \\ &+ \sum_{j=i+1}^I (K_{j-i,i}^2 + K_{j-i,i}^3) N_i^n N_j^n \Delta \omega_j - \sum_{j=1}^{i-1} (K_{i-j,j}^2 + K_{i-j,j}^3) N_i^n N_j^n \Delta \omega_j \\ &\left. + \sum_{(j,k) \in \mathcal{J}_{j,k}^i} (K_{j-k,k}^2 + K_{j-k,k}^3) N_j^n N_k^n \frac{\Delta \omega_j \Delta \omega_k}{\Delta \omega_i} \right).\end{aligned}$$

2.1. New formulation of the energy conserving scheme. Since our aim of FVS is to conserve the total energy of the system, however, the scheme (2.10) only predict the zeroth order moment but not for the conservation of the total energy of the system. However, this can be achieved by introducing the suitable weight functions into the formulation. Hence, the expression takes the following form:

$$(2.11) \quad \begin{aligned}N_i^{n+1} = N_i^n + \Delta t^n &\left(\sum_{(j,k) \in \mathcal{I}_{j,k}^i} K_{j,k}^1 N_j^n N_k^n \frac{\Delta \omega_j \Delta \omega_k}{\Delta \omega_i} \alpha_{j,k} - 2 \sum_{j=1}^I K_{i,j}^1 N_i^n N_j^n \Delta \omega_j \right. \\ &+ \sum_{j=i+1}^I (K_{j-i,i}^2 + K_{j-i,i}^3) N_i^n N_j^n \Delta \omega_j - \sum_{j=1}^{i-1} (K_{i-j,j}^2 + K_{i-j,j}^3) N_i^n N_j^n \Delta \omega_j \beta_{i,j} \\ &\left. + \sum_{(j,k) \in \mathcal{J}_{j,k}^i} (K_{j-k,k}^2 + K_{j-k,k}^3) N_j^n N_k^n \frac{\Delta \omega_j \Delta \omega_k}{\Delta \omega_i} \right).\end{aligned}$$

Where the weights $\alpha_{j,k}$ are $\beta_{i,j}$ are the weights responsible for the conservation of energy. The weights are defined as

$$\alpha_{j,k} := \begin{cases} \frac{\omega_j + \omega_k}{\omega_i}, & \text{if } \omega_j + \omega_k \leq R, \\ 0, & \text{otherwise.} \end{cases}$$

$$\beta_{i,j} := \begin{cases} \frac{2\omega_j}{\omega_i}, & \text{if } 0 < \omega_i, \omega_j \leq R, \\ 0, & \text{otherwise.} \end{cases}$$

Before proceeding to the propositions, we first impose a constraint on the kernel to ensure the mathematical validity of the numerical method. This constraint is defined as follows:

$$(2.12) \quad K^i(\omega, \mu) := \begin{cases} K^i(\omega, \mu), & \text{if } 0 < \omega + \mu \leq R \text{ and } \omega, \mu > 0, \\ 0, & \text{otherwise.} \end{cases}$$

for $i = 1, 2, 3$. This constraint is applied purely for the mathematical verification of the properties of total volume conservation and the consistency of the numerical method.

Proposition 2.1. *The proposed finite volume scheme (2.11) is energy conserving.*

Proof. The above result can be proved as follows. Multiply the discrete formulation (2.10) by $\omega_i \Delta \omega_i$ and taking sum over all i on both side, we can obtain

$$\sum_{i=1}^I \omega_i N_i^{n+1} \Delta \omega_i = \sum_{i=1}^I \omega_i N_i^n \Delta \omega_i + \Delta t^n T.$$

Where

$$\begin{aligned} T = & \sum_{i=1}^I \sum_{(j,k) \in \mathcal{I}_{j,k}^i} \omega_i K_{j,k}^1 N_j^n N_k^n \Delta \omega_j \Delta \omega_k \alpha_{j,k} - 2 \sum_{i=1}^I \sum_{j=1}^I \omega_i K_{i,j}^1 N_i^n N_j^n \Delta \omega_j \\ & + \sum_{i=1}^I \sum_{(j,k) \in \mathcal{J}_{j,k}^i} \omega_i (K_{j-k,k}^2 + K_{j-k,k}^3) N_j^n N_k^n \Delta \omega_j \Delta \omega_k \\ & - \sum_{i=2}^I \sum_{j=1}^{i-1} \omega_i (K_{i-j,j}^2 + K_{i-j,j}^3) N_i^n N_j^n \Delta \omega_i \omega_j \beta_{i,j} \\ & + \sum_{i=1}^I \sum_{j=i+1}^I \omega_i (K_{j-i,i}^2 + K_{j-i,i}^3) N_i^n N_j^n \Delta \omega_j \Delta \omega_i. \end{aligned}$$

In order to prove the energy conservation we need to show that $T = 0$. First we simplify the terms in right hand side of T .

From the definition of the weight α we have

$$\sum_{(j,k) \in \mathcal{K}_{j,k}^*} K_{j,k}^1 N_j^n N_k^n \Delta \omega_j \Delta \omega_k \alpha_{j,k} = 0.$$

Further, $\sum_{i=1}^I \sum_{j=1}^I$ represents all possible combinations of the cells i and j . Here two cases will

arise: either the sum of cell representative of the cells i and j , i.e., $\omega_i + \omega_j$ will fall either inside

or outside of the computational domain. So, we can write $\sum_{j=1}^I = \sum_{(j,k) \in \mathcal{I}_{j,k}^i} + \sum_{(j,k) \in \mathcal{K}_{j,k}^*}$. Therefore,

using this relation, the first term of T can be written as

$$(2.13) \quad \sum_{i=1}^I \sum_{(j,k) \in \mathcal{I}_{j,k}^i} K_{j,k}^1 N_j^n N_k^n \Delta \omega_j \Delta \omega_k \alpha_{j,k} = \sum_{i=1}^I \sum_{j=1}^I (\omega_i + \omega_j) K_{i,j}^1 N_i^n N_j^n \Delta \omega_i \Delta \omega_j.$$

The third term also can be simplified in the similar manner

(2.14)

$$\sum_{i=1}^I \sum_{(j,k) \in \mathcal{T}_{j,k}^i} \omega_i (K_{j-k,k}^2 + K_{j-k,k}^3) N_j^n N_k^n \Delta\omega_j \Delta\omega_k = \sum_{i=1}^I \sum_{j=i+1}^I \omega_i (K_{j-i,i}^2 + K_{j-i,i}^3) N_j^n N_i^n \Delta\omega_j \Delta\omega_i.$$

Finally, using the simplified values (2.13), (2.14) and the weight β in T .

$$\begin{aligned} T &= \sum_{i=1}^I \sum_{j=1}^I (\omega_i + \omega_j) K_{i,j}^1 N_i^n N_j^n \Delta\omega_i \Delta\omega_j - 2 \sum_{i=1}^I \sum_{j=1}^I \omega_i K_{i,j}^1 N_i^n N_j^n \Delta\omega_j \\ &\quad + \sum_{i=1}^I \sum_{j=i+1}^I \omega_i (K_{j-i,i}^2 + K_{j-i,i}^3) N_j^n N_i^n \Delta\omega_j \Delta\omega_i \\ &\quad - 2 \sum_{i=2}^I \sum_{j=1}^{i-1} \omega_j (K_{i-j,j}^2 + K_{i-j,j}^3) N_i^n N_j^n \Delta\omega_i \omega_j \\ &\quad + \sum_{i=1}^I \sum_{j=i+1}^I \omega_i (K_{j-i,i}^2 + K_{j-i,i}^3) N_i^n N_j^n \Delta\omega_j \Delta\omega_i \\ &= \sum_{i=1}^I \sum_{j=1}^I (\omega_i + \omega_j) K_{i,j}^1 N_i^n N_j^n \Delta\omega_i \Delta\omega_j - 2 \sum_{i=1}^I \sum_{j=1}^I \omega_i K_{i,j}^1 N_i^n N_j^n \Delta\omega_j \\ &\quad + \sum_{i=1}^I \sum_{j=i+1}^I \omega_i (K_{j-i,i}^2 + K_{j-i,i}^3) N_j^n N_i^n \Delta\omega_j \Delta\omega_i \\ &\quad - 2 \sum_{j=1}^I \sum_{i=j+1}^I \omega_j (K_{i-j,j}^2 + K_{i-j,j}^3) N_i^n N_j^n \Delta\omega_i \omega_j \\ &\quad + \sum_{i=1}^I \sum_{j=i}^I \omega_i (K_{j-i,i}^2 + K_{j-i,i}^3) N_i^n N_j^n \Delta\omega_j \Delta\omega_i = 0. \end{aligned}$$

Hence, the total energy of the system is conserved by the proposed scheme. \square

3. CONVERGENCE ANALYSIS OF THE FVS

Let us express the numerical approximate solution in the vector form $\hat{\mathbf{F}} := \{\hat{F}_1, \hat{F}_2, \dots, \hat{F}_I\}$ where $\hat{F}_i = \hat{N}_i \Delta\omega_i$ and \hat{N}_i be the approximate solution satisfying the following relation,

$$(3.1) \quad N_\omega = \sum_{i=1}^I F_i \delta(\omega - \omega_i) + \mathcal{O}(\Delta\omega^3).$$

We also denote the projected exact solution by $\mathbf{F} := \{F_1, F_2, \dots, F_I\}$. Then FVS (2.10) can be rewritten in the following vector form

$$(3.2) \quad \frac{d\hat{\mathbf{F}}}{dt} = \hat{\mathbf{J}}(\hat{\mathbf{F}}).$$

Here $\hat{\mathbf{J}} := \{\hat{J}_1, \hat{J}_2, \dots, \hat{J}_I\}$ is a vector in \mathbb{R}^I , whose i -th component is given by

$$(3.3) \quad \hat{J}_i(\hat{\mathbf{F}}) := \sum_{k=1}^5 \hat{Q}_i^k(\hat{\mathbf{F}}).$$

Where

$$(3.4) \quad \hat{Q}_i^1(\hat{\mathbf{F}}) := \sum_{(j,k) \in \mathcal{I}_{j,k}^i} K_{j,k}^1 \hat{F}_j(t) \hat{F}_k(t),$$

$$(3.5) \quad \hat{Q}_i^2(\hat{\mathbf{F}}) := -2 \sum_{j=1}^I K_{i,j}^1 \hat{F}_i(t) \hat{F}_j(t),$$

$$(3.6) \quad \hat{Q}_i^3(\hat{\mathbf{F}}) := \sum_{(j,k) \in \mathcal{J}_{j,k}^i} (K_{j-k,k}^2 + K_{j-k,k}^3) \hat{F}_j(t) \hat{F}_k(t),$$

$$(3.7) \quad \hat{Q}_i^4(\hat{\mathbf{F}}) := - \sum_{j=1}^{i-1} (K_{i-j,j}^2 + K_{i-j,j}^3) \hat{F}_i(t) \hat{F}_j(t),$$

$$(3.8) \quad \hat{Q}_i^5(\hat{\mathbf{F}}) := \sum_{j=i+1}^I (K_{j-i,i}^2 + K_{j-i,i}^3) \hat{F}_i(t) \hat{F}_j(t).$$

The subsequent part of this section we consider the discrete L^1 norm

$$\|\mathbf{F}(t)\| := \sum_{i=1}^I |F_i(t)|.$$

Moreover, we consider the space $\mathcal{C}^2((0, R])$, the space of twice continuous differentiable on $(0, R]$. For the sake of simplicity of our convergence analysis, we assume that the wave kernels are lies in the space $\mathcal{C}^2((0, R] \times (0, R])$, that is

$$(3.9) \quad K_i(\omega, \mu) \in \mathcal{C}^2((0, R] \times (0, R]), \quad \text{for } i = 1, 2, 3.$$

In order to prove the convergence analysis of the above defined numerical scheme, we need to define some useful definition and results from [72] and [73], which we will use in the rest of our study.

Definition 3.1. The spatial discretization error is defined by the residual from substituting the exact solution $\mathbf{F} := \{F_1, F_2, \dots, F_I\}$ into the discrete system as

$$\sigma(t) = \frac{d\mathbf{F}}{dt} - \hat{\mathbf{J}}(\mathbf{F}).$$

We will say the numerical scheme (3.2) is p -th order consistent if, $\Delta\omega \rightarrow 0$

$$(3.10) \quad \|\sigma(t)\| = \mathcal{O}(\Delta\omega^p) \quad \text{uniformly for all } 0 \leq t \leq T.$$

Now our first goal will be to prove the mapping $\hat{\mathbf{J}}$ is satisfying the Lipschitz condition with a Lipschitz constant γ which is independent of mesh. Before going to prove the Lipschitz condition, we will prove a uniform boundedness of the numerical solution in the following proposition.

Proposition 3.1. *Let the wave K_1 , K_2 and K_3 satisfies the assumption (3.9). Then there exist a positive constant $\mathcal{A}(T)$ independent of mesh satisfying the condition*

$$\|\mathbf{F}(t)\| \leq \mathcal{A}(T) \quad \text{for all } t \in [0, T].$$

Proof. Taking sum on the both side of equation (3.2) over i from 1 to I , we get

$$\begin{aligned} \frac{d}{dt} \|\mathbf{F}(t)\| &= \sum_{i=1}^I \sum_{(j,k) \in \mathcal{I}_{j,k}^i} \omega_i K_{j,k}^1 F_j(t) F_k(t) - 2 \sum_{i=1}^I \sum_{j=1}^I K_{i,j}^1 F_i(t) F_j(t) \\ &+ \sum_{i=1}^I \sum_{(j,k) \in \mathcal{J}_{j,k}^i} (K_{j-k,k}^2 + K_{j-k,k}^3) F_j(t) F_k(t) - \sum_{i=2}^I \sum_{j=1}^{i-1} (K_{i-j,j}^2 + K_{i-j,j}^3) F_i(t) F_j(t) \\ &+ \sum_{i=1}^I \sum_{j=i+1}^I (K_{j-i,i}^2 + K_{j-i,i}^3) F_i(t) F_j(t). \end{aligned}$$

Now proceed similar as Proposition 2.1 to simplify the first and third term in the right hand side of the above equation, yields

$$\begin{aligned} \frac{d}{dt} \|\mathbf{F}(t)\| &= - \sum_{i=1}^I \sum_{j=1}^I K_{i,j}^1 F_i(t) F_j(t) + \sum_{i=1}^I \sum_{j=i+1}^I (K_{j-i,i}^2 + K_{j-i,i}^3) F_j(t) F_i(t) \\ &- \sum_{i=2}^I \sum_{j=1}^{i-1} (K_{i-j,j}^2 + K_{i-j,j}^3) F_i(t) F_j(t) + \sum_{i=1}^I \sum_{j=i+1}^I (K_{j-i,i}^2 + K_{j-i,i}^3) F_i(t) F_j(t). \end{aligned}$$

Since, we assume that $K_i(\omega, \mu) \in \mathcal{C}^2((0, R] \times (0, R])$ for $i = 1, 2, 3$, so there exist a constant \mathcal{L} such that

$$(3.11) \quad \sup_{(\omega, \mu) \in (0, R]} K_i(\omega, \mu) \leq \mathcal{L}.$$

This estimation reduces the above identity into the following differential inequality

$$\frac{d}{dt} \|\mathbf{F}(t)\| \leq 2\mathcal{L} \|\mathbf{F}(t)\|^2, \quad \text{for all } 0 \leq t \leq T.$$

Hence, the uniform boundedness result directly follow from this inequality. \square

Proposition 3.2. *Assume that the wave kernels K_1 , K_2 and K_3 lies in the space $\mathcal{C}^2((0, R] \times (0, R])$. Then there exist a positive constant γ independent of mesh such that*

$$(3.12) \quad \|\hat{\mathbf{J}}(\mathbf{F}) - \hat{\mathbf{J}}(\hat{\mathbf{F}})\| \leq \gamma \|\mathbf{F} - \hat{\mathbf{F}}\|, \quad \text{for all } \mathbf{F}, \hat{\mathbf{F}} \in \mathbb{R}^I.$$

Proof. In order to prove the mapping $\hat{\mathbf{J}}$ defined in (3.3) satisfy the Lipschitz condition, we will show that each of the term \hat{Q}^k ($k = 1, \dots, 5$) is satisfying the Lipschitz condition. Let, $\mathbf{F}, \hat{\mathbf{F}} \in \mathbb{R}^I$,

$$\|\hat{Q}^1(\mathbf{F}) - \hat{Q}^1(\hat{\mathbf{F}})\| = \sum_{i=1}^I \left| \hat{Q}_i^1(\mathbf{F}) - \hat{Q}_i^1(\hat{\mathbf{F}}) \right| = \sum_{i=1}^I \sum_{(j,k) \in \mathcal{I}_{j,k}^i} |K_{j,k}^1| \left| F_j F_k - \hat{F}_j \hat{F}_k \right|.$$

Now one can observe the following fact

$$(3.13) \quad \left| F_j F_k - \hat{F}_j \hat{F}_k \right| = \frac{1}{2} \left| (F_j + \hat{F}_j) (F_k - \hat{F}_k) + (F_j - \hat{F}_j) (F_k + \hat{F}_k) \right|.$$

Using the Proposition 3.1 together with condition (3.11) and identity (3.13) on the above norm reduce to

$$\begin{aligned} \|\hat{Q}^1(\mathbf{F}) - \hat{Q}^1(\hat{\mathbf{F}})\| &\leq \frac{\mathcal{L}}{2} \sum_{j=1}^I \sum_{k=1}^I \left| (F_j + \hat{F}_j)(F_k - \hat{F}_k) + (F_j - \hat{F}_j)(F_k + \hat{F}_k) \right| \\ &\leq 2\mathcal{L}\mathcal{A}(T)\|\mathbf{F} - \hat{\mathbf{F}}\|. \end{aligned}$$

Similar process can be follow to show the remaining terms that is \hat{Q}^k ($k = 2, \dots, 5$) are also satisfies the Lipschitz condition. And substitute all these estimations in the following identity

$$\|\hat{\mathbf{J}}(\mathbf{F}) - \hat{\mathbf{J}}(\hat{\mathbf{F}})\| = \sum_{k=1}^5 \|\hat{Q}^k(\mathbf{F}) - \hat{Q}^k(\hat{\mathbf{F}})\|.$$

we can get a constant γ which is depending only on T and \mathcal{L} not on the choice of mesh such that the inequality (3.12) holds. \square

Now we are in the stage where we can start proving our main convergence theorem.

Theorem 3.1. *Let the wave interaction kernels K_i ($i = 1, 2, 3$) are belongs to the space $\mathcal{C}^2((0, R] \times (0, R])$. Then the proposed finite volume scheme (3.2) is nonnegative and consistent with first order consistency. Consequently, the numerical scheme (3.2) is convergent and the order of convergence is the same of order of consistency.*

Proof. To prove the convergence of the proposed finite volume scheme (3.2), our next goal is to demonstrate that the numerical scheme is both nonnegative and consistent. To begin, we show that the scheme is nonnegative.

Nonnegativity: Consider any nonnegative approximate solution $\hat{\mathbf{F}} = \{\hat{F}_1, \hat{F}_2, \dots, \hat{F}_I\}$ for which the i -th component $\hat{F}_i = 0$. Then from the definition of the numerical fluxes (3.4)-(3.8), we can get $\hat{Q}_i^1(\hat{\mathbf{F}}) \geq 0$, $\hat{Q}_i^2(\hat{\mathbf{F}}) = 0$, $\hat{Q}_i^3(\hat{\mathbf{F}}) \geq 0$, $\hat{Q}_i^4(\hat{\mathbf{F}}) = 0$ and $\hat{Q}_i^5(\hat{\mathbf{F}}) = 0$. Therefore, using these relations in (3.3), we get $\hat{J}_i(\hat{\mathbf{F}}) \geq 0$ for any $i \in \{1, 2, \dots, I\}$, moreover, $\hat{\mathbf{J}}$ is Lipschitz from Proposition 3.2. Then thanks to the Theorem 4.1 of [72], we can say that our proposed FVS is nonnegative.

Consistency: To prove the consistency of the proposed scheme (3.2), we need to calculate the discretization error for each of the terms (3.4)-(3.8). Let us start from the first term and then change the order of the integration

$$\begin{aligned} Q_i^1(t) &= \int_{\omega_{i-1/2}}^{\omega_{i+1/2}} \int_0^\omega K_1(\omega - \mu, \mu) N_{\omega-\mu}(t) N_\mu(t) d\mu d\omega \\ &= \left[\int_{\omega_{i-1/2}}^{\omega_{i+1/2}} \int_0^{\omega_{i-1/2}} + \int_{\omega_{i-1/2}}^{\omega_{i+1/2}} \int_{\omega_{i-1/2}}^\omega \right] K_1(\omega - \mu, \mu) N_{\omega-\mu}(t) N_\mu(t) d\mu d\omega \\ &= \left[\int_{\omega_{i-1/2}}^{\omega_{i+1/2}} \sum_{j=1}^{i-1} \int_{\omega_{j-1/2}}^{\omega_{j+1/2}} + \int_{\omega_{i-1/2}}^{\omega_{i+1/2}} \int_{\omega_{i-1/2}}^\omega \right] K_1(\omega - \mu, \mu) N_{\omega-\mu}(t) N_\mu(t) d\mu d\omega. \end{aligned}$$

On applying the relation (3.1) for the midpoint quadrature rule on the above equation and we get $Q_i^1(t)$ in the following form,

$$\begin{aligned}
Q_i^1 &= \sum_{j=1}^{i-1} \int_{\omega_{i-1/2}}^{\omega_{i+1/2}} \int_{\omega_{j-1/2}}^{\omega_{j+1/2}} K_1(\omega - \mu, \mu) \sum_{k=1}^I F_k(t) \delta(\omega - \mu - \omega_k) \sum_{l=1}^I F_l(t) \delta(\mu - \omega_l) d\mu d\omega \\
&\quad + \int_{\omega_{i-1/2}}^{\omega_{i+1/2}} \int_{\mu}^{\omega_{i+1/2}} K_1(\omega - \mu, \mu) \sum_{k=1}^I F_k(t) \delta(\omega - \mu - \omega_k) \sum_{l=1}^I F_l(t) \delta(\mu - \omega_l) d\omega d\mu + \mathcal{O}(\Delta\omega^3) \\
&= \sum_{j=1}^{i-1} F_j(t) \int_{\omega_{i-1/2}}^{\omega_{i+1/2}} K_1(\omega - \omega_j, \omega_j) \sum_{k=1}^I F_k(t) \delta(\omega - \omega_j - \omega_k) d\mu \\
&\quad + F_i(t) \int_{\omega_i}^{\omega_{i+1/2}} K_1(\omega - \omega_i, \omega_i) \sum_{k=1}^I F_k(t) \delta(\omega - \omega_i - \omega_k) d\mu + \mathcal{O}(\Delta\omega^3) \\
&= \sum_{j=1}^{i-1} \sum_{\omega_{i-1/2} \leq \omega_j + \omega_k < \omega_{i+1/2}} K_{j,k}^1 F_j(t) F_k(t) + F_i(t) \Delta\omega_i \sum_{\omega_i + \omega_k < \omega_{i+1/2}} K_{i,k}^1 F_k(t) + \mathcal{O}(\Delta\omega^3) \\
&= \sum_{(j,k) \in \mathcal{I}_{j,k}^i} K_{j,k}^1 F_j(t) F_k(t) + \mathcal{O}(\Delta\omega^3) \\
&= \hat{Q}_i^1(\mathbf{F}) + \mathcal{O}(\Delta\omega^3).
\end{aligned}$$

Using the simple application of midpoint quadrature rule, we can discretize the second term as follows

$$\begin{aligned}
Q_i^2 &= -2 \int_{\omega_{i-1/2}}^{\omega_{i+1/2}} \sum_{j=1}^I \int_{\omega_{j-1/2}}^{\omega_{j+1/2}} K_1(\omega, \mu) N_\omega(t) N_\mu(t) d\mu d\omega \\
&= -2 \int_{\omega_{i-1/2}}^{\omega_{i+1/2}} \sum_{k=1}^I F_k(t) \delta(\omega - \omega_k) \sum_{j=1}^I \int_{\omega_{j-1/2}}^{\omega_{j+1/2}} K_1(\omega, \mu) \sum_{k=1}^I F_k(t) \delta(\mu - \omega_k) d\mu d\omega + \mathcal{O}(\Delta\omega^3) \\
&= -2 \sum_{j=1}^I K_{i,j}^1 F_i(t) F_j(t) + \mathcal{O}(\Delta\omega^3) \\
&= \hat{Q}_i^2(\mathbf{F}) + \mathcal{O}(\Delta\omega^3).
\end{aligned}$$

To find the discretization error in the term Q_i^3 , we first substitute $\mu = \mu' - \omega$ in the second integral of (2.6) then replace μ' by μ .

$$Q_i^3(t) = \int_{\omega_{i-1/2}}^{\omega_{i+1/2}} \int_{\omega}^R [K_2(\omega, \mu - \omega) + K_3(\omega, \mu - \omega)] N_{\mu-\omega} N_{\mu} d\omega.$$

Then proceed similar as $Q_i^1(t)$ above, the reduced form of $Q_i^3(t)$ can be written as follows

$$\begin{aligned}
Q_i^3 &= \int_{\omega_{i-1/2}}^{\omega_{i+1/2}} \sum_{j=i+1}^I \int_{\omega_{j-1/2}}^{\omega_{j+1/2}} [K_2(\omega, \mu - \omega) + K_3(\omega, \mu - \omega)] N_{\mu-\omega} N_{\mu} d\mu d\omega \\
&\quad + \int_{\omega_{i-1/2}}^{\omega_{i+1/2}} \int_{\omega}^{\omega_{i+1/2}} [K_2(\omega, \mu - \omega) + K_3(\omega, \mu - \omega)] N_{\mu-\omega} N_{\mu} d\mu d\omega
\end{aligned}$$

$$\begin{aligned}
&= \sum_{j=i+1}^I F_j(t) \int_{\omega_{i-1/2}}^{\omega_{i+1/2}} [K_2(\omega, \omega_j - \omega) + K_3(\omega, \omega_j - \omega)] \sum_{k=1}^I F_k(t) \delta(\omega_j - \omega - \omega_k) d\omega \\
&\quad + F_i(t) \int_{\omega_{i-1/2}}^{\omega_i} K_2(\omega, \omega_i - \omega) \sum_{k=1}^I F_k(t) \delta(\omega_i - \omega - \omega_k) d\omega + \mathcal{O}(\Delta\omega^3) \\
&= \sum_{j=i+1}^I \sum_{\omega_{i-1/2} \leq \omega_j - \omega_k < \omega_{i+1/2}} [K_{j-k,k}^2 + K_{j-k,k}^3] F_j(t) F_k(t) \\
&\quad + \sum_{\omega_{i-1/2} \leq \omega_i - \omega_k} [K_{i-k,k}^2 + K_{i-k,k}^3] F_i(t) F_k(t) + \mathcal{O}(\Delta\omega^3) \\
&= \sum_{(j,k) \in \mathcal{J}_{j,k}^i} K_{j-k,k}^2 F_j(t) F_k(t) \Delta\omega_j \Delta\omega_k + \mathcal{O}(\Delta\omega^3) \\
&= \hat{Q}_i^3(\mathbf{F}) + \mathcal{O}(\Delta\omega^3).
\end{aligned}$$

To obtain the discretization error of the fourth term we substitute $\mu = \omega - \mu'$ in the second integral of (2.7) then replace μ' by μ .

$$\begin{aligned}
\mathcal{Q}_i^4 &= - \int_{\omega_{i-1/2}}^{\omega_{i+1/2}} \int_0^\omega [K_2(\mu, \omega - \mu) + K_3(\mu, \omega - \mu)] N_\omega(t) N_\mu(t) d\mu d\omega \\
&= F_i(t) \int_0^{\omega_i} [K_2(\mu, \omega - \mu) + K_3(\mu, \omega - \mu)] \sum_{k=1}^I F_k(t) \delta(\mu - \omega_k) d\mu + \mathcal{O}(\Delta\omega^3) \\
&= -F_i(t) \sum_{j=1}^{i-1} \int_{\omega_{j-1/2}}^{\omega_{j+1/2}} [K_2(\mu, \omega_i - \mu) + K_3(\mu, \omega_i - \mu)] \sum_{k=1}^I F_k(t) \delta(\mu - \omega_k) d\mu \\
&\quad - F_i(t) \int_{\omega_{i-1/2}}^{\omega_i} [K_2(\mu, \omega_i - \mu) + K_3(\mu, \omega_i - \mu)] \sum_{k=1}^I F_k(t) \delta(\mu - \omega_k) d\mu + \mathcal{O}(\Delta\omega^3) \\
&= - \sum_{j=1}^{i-1} [K_{i-j,j}^2 + K_{i-j,j}^3] F_i F_j \\
&\quad - F_i(t) \int_{\omega_{i-1/2}}^{\omega_i} [K_2(\mu, \omega_i - \mu) + K_3(\mu, \omega_i - \mu)] \sum_{k=1}^I F_k(t) \delta(\mu - \omega_k) d\mu + \mathcal{O}(\Delta\omega^3) \\
&= \hat{Q}_i^4(\mathbf{F}) - E_1 + \mathcal{O}(\Delta\omega^3).
\end{aligned}$$

Where

$$E_1 = F_i(t) \int_{\omega_{i-1/2}}^{\omega_i} [K_2(\mu, \omega_i - \mu) + K_3(\mu, \omega_i - \mu)] \sum_{k=1}^I F_k(t) \delta(\mu - \omega_k) d\mu.$$

Now apply the right end quadrature rule on the integral of E_1 and using the condition (2.12) on the wave interaction kernel K_2 and K_3 . Then the integral term E_1 reduce to $E_1 = \mathcal{O}(\Delta\omega^2)$. Therefore, $\mathcal{Q}_i^4(\mathbf{F}) = \hat{Q}_i^4(\mathbf{F}) + \mathcal{O}(\Delta\omega^2)$.

For the final term, we first substitute $\mu' = \omega + \mu$ on the first integral of (2.8) and replace μ' by μ .

$$\begin{aligned}
Q_i^5 &= \int_{\omega_{i-1/2}}^{\omega_{i+1/2}} \int_{\omega}^R [K_2(\omega, \mu - \omega) + K_3(\omega, \mu - \omega)] N_{\omega}^n N_{\mu}^n d\mu d\omega \\
&= F_i(t) \sum_{j=i+1}^I \int_{\omega_{j-1/2}}^{\omega_{j+1/2}} [K_2(\omega_i, \mu - \omega_i) + K_3(\omega_i, \mu - \omega_i)] \sum_{k=1}^I F_k(t) \delta(\mu - \omega_k) d\mu \\
&\quad + F_i(t) \int_{\omega_i}^{\omega_{i+1/2}} [K_2(\omega_i, \mu - \omega_i) + K_3(\omega_i, \mu - \omega_i)] \sum_{k=1}^I F_k(t) \delta(\mu - \omega_k) d\mu + \mathcal{O}(\Delta\omega^3) \\
&= \sum_{j=i}^I [K_{j-i,i}^2 + K_{j-i,i}^3] F_i(t) F_j \\
&\quad + F_i(t) \int_{\omega_i}^{\omega_{i+1/2}} [K_2(\omega_i, \mu - \omega_i) + K_3(\omega_i, \mu - \omega_i)] \sum_{k=1}^I F_k(t) \delta(\mu - \omega_k) d\mu + \mathcal{O}(\Delta\omega^3) \\
&= \hat{Q}_i^5(\mathbf{F}) + E_2 + \mathcal{O}(\Delta\omega^3).
\end{aligned}$$

Where

$$E_2 = F_i(t) \int_{\omega_i}^{\omega_{i+1/2}} [K_2(\omega_i, \mu - \omega_i) + K_3(\omega_i, \mu - \omega_i)] \sum_{k=1}^I F_k(t) \delta(\mu - \omega_k) d\mu.$$

Apply the right end quadrature rule on the integral of E_1 and using the condition (2.12) on the wave interaction kernel K_2 and K_3 . Then the integral term E_1 reduce to $E_2 = \mathcal{O}(\Delta\omega^2)$. Finally we get the discretization error of the last term as follow $Q_i^5(\mathbf{F}) = \hat{Q}_i^5(\mathbf{F}) + \mathcal{O}(\Delta\omega^2)$.

Now using all these obtained discretization error value in the Definition 3.1, we can obtain the spatial discretization error

$$\sigma_i = \left| J_i(\mathbf{F}) - \hat{J}_i(\mathbf{F}) \right| = \sum_{k=1}^5 \left| Q_i^k(\mathbf{F}) - \hat{Q}_i^k(\mathbf{F}) \right| = \mathcal{O}(\Delta\omega^2).$$

This further implies $\|\sigma\| = \sum_{i=1}^I |\sigma_i(t)| = \mathcal{O}(\Delta\omega)$.

Convergence: To conclude the convergence proof, we combine these above results with the Proposition 3.2, which fulfill all the necessary conditions of the convergence analysis of [73]. Hence, the proposed finite volume scheme (3.2) is convergent. Moreover, the scheme is first order convergent as same as the order of consistency. \square

4. NUMERICAL TEST

To test our numerical schemes, we will rely on the theoretical work [74], in which the authors demonstrate that the solution to the fully nonlinear coagulation-fragmentation model exhibits a property where energy cascades from small wave numbers to large wave numbers in the capacity case. More precisely, they prove that the energy on the interval $[0, \infty)$ is a non-increasing function in time. That is for all $T_1 > 0$ we can always find a larger time $T_2 > T_1$ such that

$$(4.1) \quad \int_0^{\infty} \omega N_{\omega}(T_2) d\omega < \int_0^{\infty} \omega N_{\omega}(T_1) d\omega.$$

They also decompose the energy of a solution $g_\omega(t) = \omega N_\omega(t)$ at any time t as follows

$$(4.2) \quad g_\omega(t) = \bar{g}_\omega(t) + \tilde{g}(t)\delta_{\{\omega=\infty\}}.$$

Where the nonnegative function \bar{g} is the regular part and \tilde{g} be the singular part which is measure, characterized by the properties $\bar{g}_\omega(0) = g_\omega(0)$ and $\tilde{g}(0) = 0$. This indicates that initially, the energy is concentrated in the regular part, and as time progresses, energy gradually accumulates at $\{\omega = \infty\}$. In this context, there exist a positive time t_1^* known as *first blow-up time* for which $\tilde{g}(t) > 0$ for all $t > t_1^*$. Moreover, after the first blow-up time there exist *infinitely many blow-up time* represented by the sequence $0 < t_1^* < t_2^* < \dots < t_n^* < \dots$, satisfying $\bar{g}_\omega(t_1^*) > \bar{g}_\omega(t_2^*) > \dots > \bar{g}_\omega(t_n^*) > \dots$ and $\tilde{g}(t_1^*) < \tilde{g}(t_2^*) < \dots < \tilde{g}(t_n^*) < \dots$. If we consider $\chi_{[0,R]}(\omega)$ be a cutt-off function of ω in the finite domain $[0, R]$, the equivalent form of the multiple blow-up time phenomena with the decay rate $\mathcal{O}\left(\frac{1}{\sqrt{t}}\right)$ can be represented for arbitrary truncation parameter R ,

$$(4.3) \quad \int_0^R \omega N_\omega(t) d\omega = \int_{\mathbb{R}_+} \chi_{[0,R]}(\omega) \omega N_\omega d\omega \leq \mathcal{O}\left(\frac{1}{\sqrt{t}}\right), \quad \text{as } t \rightarrow \infty.$$

Our finite volume scheme allows for the numerical observation of the multiple blow-up time phenomenon, $t_1^* < t_2^* < \dots < t_n^* < \dots$, as well as the verification of the energy decay rate estimate given by (4.3) for the fully nonlinear coagulation-fragmentation model (1.3).

We consider some test problems to compare the efficiency of the newly proposed finite volume schemes (2.10) and (2.11) with the theoretical results of [74]. We solve the fully nonlinear coagulation-fragmentation model using both schemes (2.10) and (2.11) for different initial conditions. For the test problems, we consider the collision kernels of the form $K_1(\omega, \mu) = (\omega\mu)^\theta$, $K_2(\omega, \mu) = (\omega\mu)^\gamma$, and $K_3(\omega, \mu) = (\omega\mu)^\delta$, where θ, γ and δ are non-negative parameters referred to as the degrees of homogeneity of the collision kernels. In each test case, we either vary the degree of homogeneity of the collision kernels while holding the truncation parameter fixed at $R = 100$, or we vary the the truncation parameter R while keeping the degree of homogeneity fixed at $\theta = \gamma = \delta = 1$. Moreover, while changing the truncation parameter, we also examine the behavior of the solution under varying or fixed numbers of grid points.

In each of the test problems, the computation time domain is taken as $[0, 1000]$ with the time step $\Delta t = 0.1$, for the final time $T = 1000$. Moreover, all the tests were performed on a uniform grid. We observe that the choice of the step length h also depends on the initial condition N_ω^{in} . The first test uses a step length $h = 0.5$ for the weighted scheme and $h = 1$ for finite volume scheme without any weight function. However, the non-weighted scheme also performed similarly for $h = 0.5$. In the second test problem, we chose $h = 0.5$ to implement our proposed FVS.

4.1. Test case I. In the first test problem, we consider an *analytical initial condition* is given by

$$(4.4) \quad N_\omega^{in} = 1.25\omega e^{-100(\omega-0.25)^2}, \quad \omega \geq 0.$$

We begin implementing the FVS (2.10) with the specific case where the degree of homogeneity satisfies $\theta = \gamma = \delta$. Specifically, we consider the nonlinear collision kernels given by

$$(4.5) \quad K_1(\omega, \mu) = K_2(\omega, \mu) = K_3(\omega, \mu) = (\omega\mu)^\theta$$

and the computation domain as $[0, 100]$. With the above setup, we plot the initial state N_ω^{in} in Figure 1a and the final state $N_\omega(T)$ in Figure 1b corresponding to the collision kernels for $\theta = 1$ in (4.5). According to the theoretical results, the energy on any finite interval tends to 0; as follows:

$$(4.6) \quad \lim_{t \rightarrow \infty} N_\omega(t) \chi_{[0, R]}(\omega) = 0.$$

Both Figures 1a and 1b successfully verify the theoretical result (4.6) proved in [74].

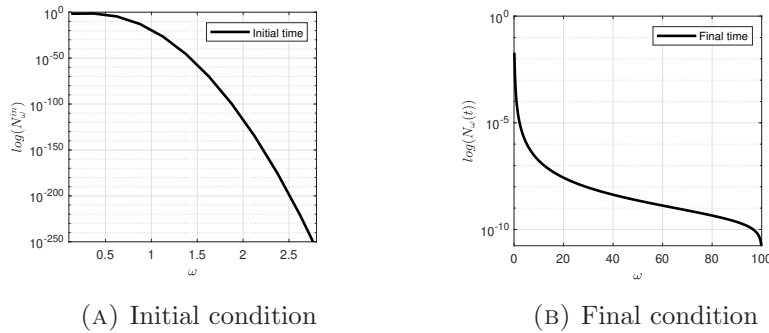


FIGURE 1. Evolution of wave density N_ω at initial and final time.

Under the consideration of the initial data (4.4) with the collision kernels (4.5), the time evolution of the first three moments $M_1(t)$, $M_2(t)$ and $M_3(t)$ is plotted for different degrees of the collision kernel: $\theta = 1, 0.85, 0.75$. The numerical approximations in Figure 2 also support the theoretical result (4.6), indicating that the wave density decays to 0 with respect to the dimensionless time t .

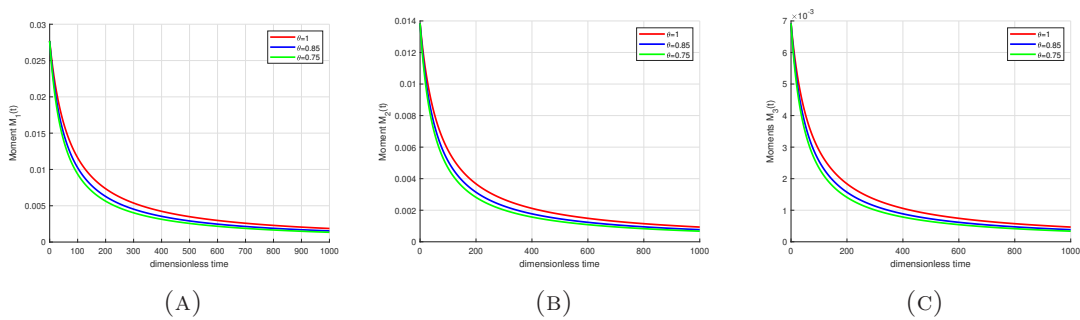
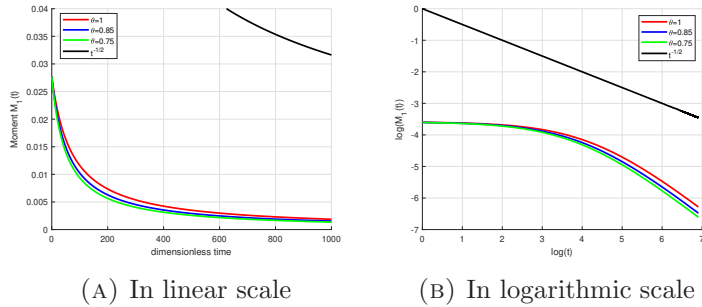
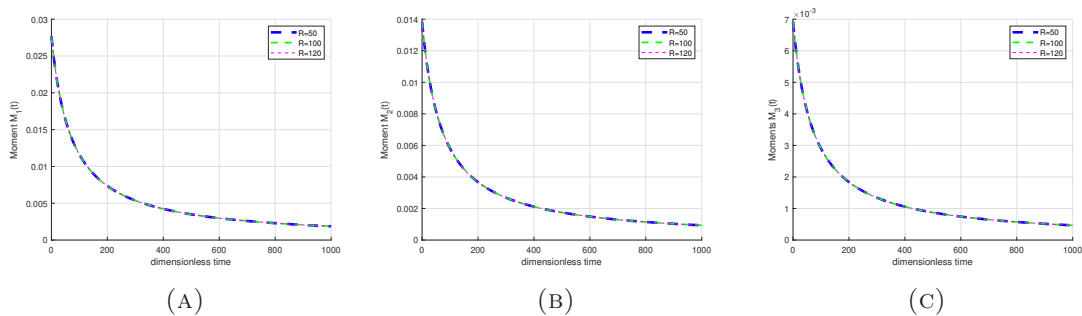


FIGURE 2. Time evolution of the (A) first, (B) second, and (C) third moments for different degrees of homogeneity θ with the same truncation parameter R .

As observed from Figure 2a, the total energy is not conserved throughout the time domain. To investigate the theoretical decay rate of the total energy in $[0, \infty)$, Figure 3 shows the total energy for different degrees θ together with the estimation given in (4.3). Figure 3 demonstrates that the theoretical result (4.3) is in very good agreement with the numerical results, where the slope of the decay rate curve is below the slope line corresponding to $\frac{1}{\sqrt{t}}$.

FIGURE 3. Decay of total energy for different values of θ .

With the same consideration of the initial data (4.4) and collision kernels (4.5), we plot the time evolution of three different moments, $M_1(t)$, $M_2(t)$ and $M_3(t)$ for three different truncation parameters, $R = 50, 100$ and 120 for a fixed degree of homogeneity $\theta = 1$. However, note that in this experiment, we maintain the same mesh length by increasing the number of grid points. From Figure 4, we can observe that the solution is not affected by the change in truncation parameter R for the same value of h .

FIGURE 4. Time evolution of the (A) first, (B) second, and (C) third moments for different truncation parameters R with the same step length h and degree of homogeneity θ .

Now, we plot the first three moment functions for different truncation parameters while keeping the degree of the collision kernel and the number of grid points fixed. This implies that, while changing the truncation parameter, the length of the sub-intervals of the mesh is also changed. We perform this experiment using 100 grid points. From Figures 5, we observe that, since the length of the sub-intervals changes, the initial evolution also changes. However, after a period of time, the solutions converge to the same pattern throughout the evolution period. This phenomenon indicates that the scheme is quite stable with respect to the step length h .

Now, we test the performance of our scheme for different collision kernels in the coagulation and fragmentation parts by choosing different degrees of homogeneity. In this regard, we choose the collision kernels as $K_1(\omega, \mu) = (\omega\mu)^\theta$, $K_2(\omega, \mu) = (\omega\mu)^\gamma$, and $K_3(\omega, \mu) = (\omega\mu)^\delta$. We plot the time evolution of three different moments for various values of θ, γ and δ in Figure 6. To conserve the total energy, we have implemented our proposed weighted FVS (2.11) for the same initial data (4.4) and set $\theta = \gamma = \delta = 0.15, 0.10, 0.05$. As discussed in the theoretical work [74], in this case, the energy cascade phenomenon (4.3) does not happen. Therefore, we expect to see a conservation of the energy of the numerical solutions. To observe the accuracy of

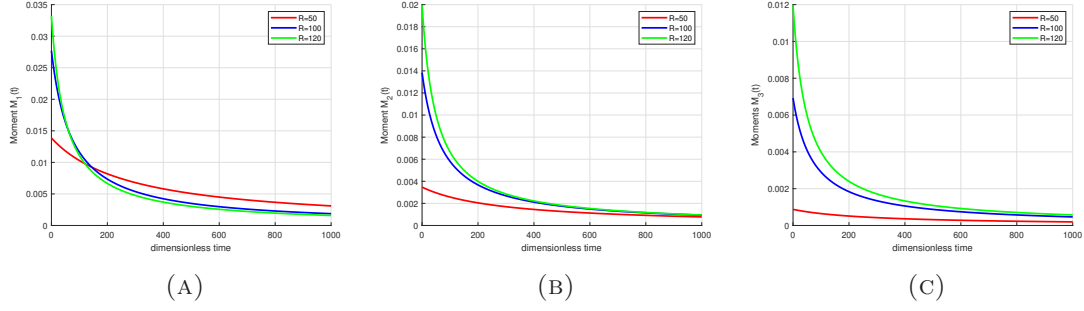


FIGURE 5. Time evolution of the (A) first, (B) second, and (C) third moments for different truncation parameters R and step lengths h with the same degree of homogeneity θ .

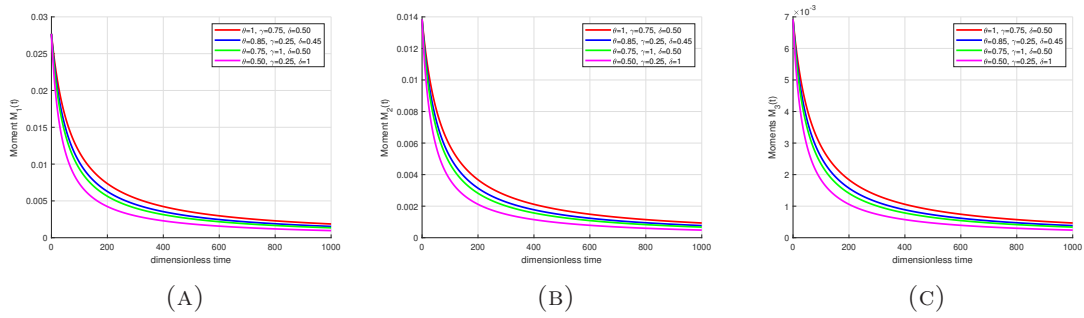


FIGURE 6. Time evolution of the (A) first, (B) second, and (C) third moments for different values of θ , γ and δ with the same truncation parameter R .

the scheme (2.11), we plot the three moment functions $M_1(t)$, $M_2(t)$ and $M_3(t)$ for different degrees of homogeneity with respect to the dimensionless time t . From Figure 7a, we can see that the first-order moment remains constant throughout the time domain. This implies that our proposed scheme (2.11) successfully conserves energy for a quite large time domain. From Figures 7b and 7c, we can observe that the second- and third-order moment functions $M_2(t)$, $M_3(t)$ show a tendency to stabilize after a short period of time.

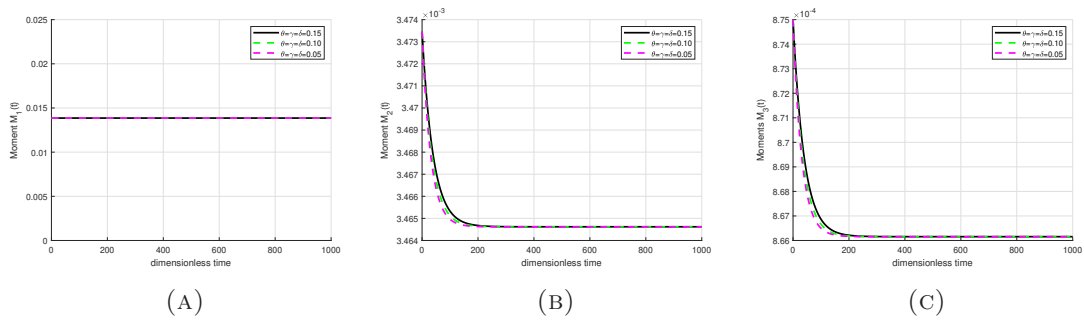


FIGURE 7. Time evolution of the (A) first, (B) second, and (C) third moments for different values of θ with the same truncation parameter R .

4.2. **Test case II:** The second numerical test employs an initial condition that is compactly supported at lower frequencies and is given by

$$(4.7) \quad N_{\omega}^{in} = \begin{cases} \exp\left(\frac{5}{|\omega-5|^2-1}\right), & \text{if } |\omega-5| \leq 1 \\ 0, & \text{if } |\omega-5| > 1. \end{cases}$$

To compute the solution, we consider the step length of the mesh points to be $h = 0.5$ with the computation domain $[0, 70]$. The initial condition and final state can be seen in Figure 8 for the collision kernels (4.5). In Figures 8a and 8b, we observe that the energy is pushed slightly toward the origin at some $T_s \in [0, T)$ to $\omega = 0.2512$, away from its initial concentration at $\omega = 4.7738$ at $t = 0$.

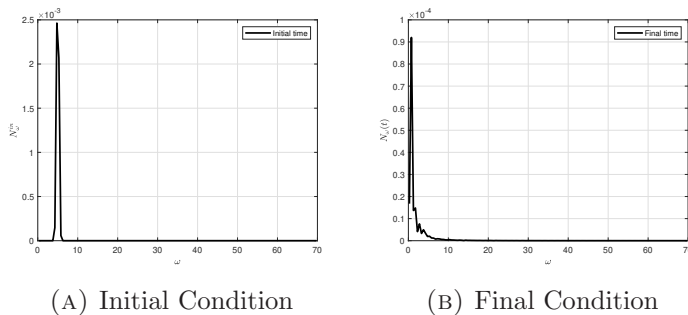


FIGURE 8. Evolution of wave density N_{ω} using the FVS (2.10) at the initial and final times.

In Figure 9, we have plotted the first three moment functions while allowing the degree of homogeneity of the collision kernels (4.5) to vary, while holding the truncation parameter fixed. We observe the decaying behavior of the total energy, as well as the other moments, similar to that in the previous test case.

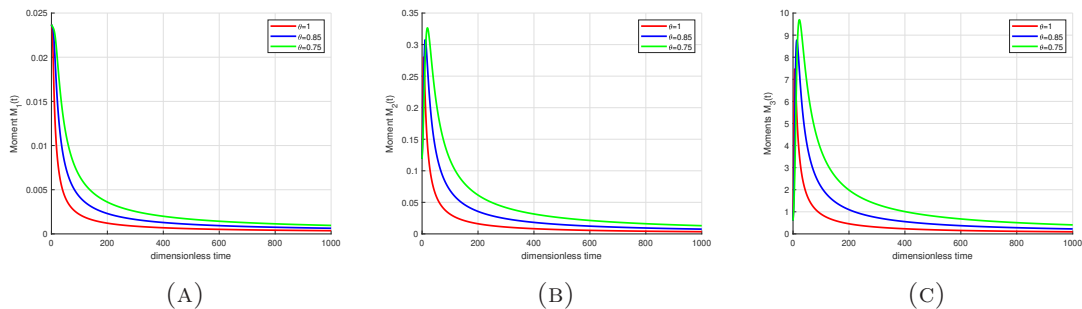
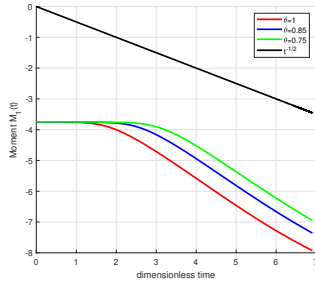


FIGURE 9. Time evolution of the (A) first, (B) second, and (C) third moments for different values of θ with the same truncation parameter R .

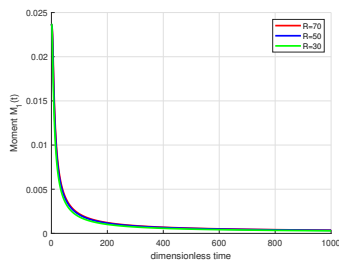
In Figure 10, the theoretical decay rate is compared with the decay of total energy for all considered values of θ . The plot indicates that the total energy in the finite interval considered is conserved for a short time, as given in [74]. After this time, the total energy in the interval begins to decay rapidly. As in the previous test cases, the numerical results show good agreement with the theoretical findings of [74]. The figure suggests that the decay is bounded by $\mathcal{O}\left(\frac{1}{\sqrt{t}}\right)$, as shown in (4.3).



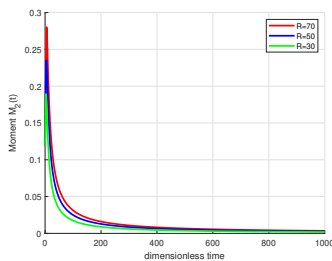
(A)

FIGURE 10. Decay of total energy for different values of θ on a logarithmic scale.

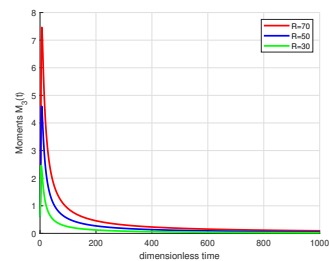
We also perform the evolution of the moment functions in Figure 11, when $\theta = 1$ is fixed and the truncation parameter R is varying. In contrast to Figure 4 in the previous test case, the differences in moments are more distinguishable. However, as already mentioned, this is consistent with the previous analysis in [74].



(A)



(B)



(C)

FIGURE 11. Time evolution of the (A) first, (B) second, and (C) third moments for different truncation parameter R with the same degree of homogeneity θ .

4.3. Experimental order of convergence. To validate the theoretical result on the order of convergence proved in the previous section, we conduct several numerical test problems to compute the *Experimental Order of Convergence* (EOC). Specifically, we calculate the EOC for the first test case (4.1) and second test case (4.2), both involving wave interaction kernels with a homogeneity degree of one. Since the exact solution for the fully nonlinear coagulation-fragmentation model equation (1.3) is not available in the literature for either test case, we compute the EOC numerically using the following formula:

$$EOC = \ln \left(\frac{\|N_I - N_{2I}\|}{\|N_{2I} - N_{4I}\|} \right) / \ln(2).$$

Here N_I denotes the approximate solution obtained by the FVS on a mesh with I number of grid points. We perform both test cases on uniform and nonuniform grids, using a geometric grid for the nonuniform case. The geometric grid is derived from the smooth transformation $\omega = \exp(\xi)$, where ξ is a variable with a uniform mesh in the computational domain $[\ln(1e - 8), \ln(2)]$ and $[\ln(1e - 8), \ln(10)]$ for the first and second test case, respectively. Additionally, the simulations are run till time $t = 200$ and $t = 50$ with time step $\Delta t = 0.1$, for the Test case 4.1 and Test case 4.2, respectively.

The table 1 provides information of the L^1 error and EOC for the initial data considered in the Test case 4.1. From this we can observe that our proposed FVS has first order convergence on uniform as well as nonuniform grid. Which is a good agreement with the theoretical proof of convergence analysis stated in Theorem 3.1.

Grid points	Uniform grids		Nonuniform grids	
	L^1 error	EOC	L^1 error	EOC
60	9.72E-4	0	6.14E-3	0
120	4.54E-4	1.0972	2.61E-3	1.2333
240	2.37E-4	0.9366	1.18E-3	1.1401
480	1.22E-4	0.9571	3.63E-4	1.0038

TABLE 1. Error and EOC for the Test case 4.1.

Grid points	Uniform grids		Nonuniform grids	
	L^1 error	EOC	L^1 error	EOC
60	3.44E-5	0	4.96E-4	0
120	1.95E-5	0.8205	4.95E-4	0.1130
240	1.04E-5	0.9107	3.09E-4	0.6784
480	5.36E-6	0.9478	1.61E-4	0.9377

TABLE 2. Error and EOC for the Test case 4.2.

In the second test case, we compute the L^1 error and EOC for the initial data considered in Test Case 4.2. The errors and EOC values for both uniform and nonuniform meshes are presented in Table 2. From the results, it can be observed that, similar to the first test case, the second test case also demonstrates first-order convergence of the FVS. This further verifies the theoretical result under favorable conditions.

REFERENCES

- [1] R. Peierls, Zur kinetischen theorie der wärmeleitung in kristallen, *Annalen der Physik* 395 (8) (1929) 1055–1101.
- [2] D. Benney, P. G. Saffman, Nonlinear interactions of random waves in a dispersive medium, *Proceedings of the Royal Society of London. Series A. Mathematical and Physical Sciences* 289 (1418) (1966) 301–320.
- [3] V. Zakharov, N. Filonenko, Weak turbulence of capillary waves, *Journal of applied mechanics and technical physics* 8 (5) (1967) 37–40.
- [4] D. Benney, A. C. Newell, Random wave closures, *Studies in Applied Mathematics* 48 (1) (1969) 29–53.
- [5] K. Hasselmann, On the non-linear energy transfer in a gravity-wave spectrum part 1. general theory, *Journal of Fluid Mechanics* 12 (4) (1962) 481–500.
- [6] K. Hasselmann, On the spectral dissipation of ocean waves due to white capping, *Boundary-Layer Meteorology* 6 (1974) 107–127.
- [7] S. Nazarenko, *Wave turbulence*, Vol. 825, Springer, 2011.
- [8] Y. Pomeau, M.-B. Tran, *Statistical physics of non equilibrium quantum phenomena*, Springer, 2019.
- [9] V. E. Zakharov, V. S. L'vov, G. Falkovich, *Kolmogorov spectra of turbulence I: Wave turbulence*, Springer Science & Business Media, 2012.
- [10] J. Banasiak, W. Lamb, P. Laurençot, *Analytic Methods for Coagulation-Fragmentation Models, Volume I*, Chapman and Hall/CRC, 2019.
- [11] J. A. Cañizo, L. Desvillettes, K. Fellner, Regularity and mass conservation for discrete coagulation–fragmentation equations with diffusion, in: *Annales de l’IHP Analyse non linéaire*, Vol. 27, 2010, pp. 639–654.

- [12] I. Cristian, M. A. Ferreira, E. Franco, J. J. Velázquez, Long-time asymptotics for coagulation equations with injection that do not have stationary solutions, *Archive for Rational Mechanics and Analysis* 247 (6) (2023) 103.
- [13] I. Cristian, J. J. Velázquez, Fast fusion in a two-dimensional coagulation model, *Journal de Mathématiques Pures et Appliquées* 184 (2024) 91–117.
- [14] P. Degond, J.-G. Liu, R. L. Pego, Coagulation–fragmentation model for animal group-size statistics, *Journal of Nonlinear Science* 27 (2017) 379–424.
- [15] M. Escobedo, P. Laurençot, S. Mischler, B. Perthame, Gelation and mass conservation in coagulation-fragmentation models, *Journal of Differential Equations* 195 (1) (2003) 143–174.
- [16] H. Liu, R. Gropler, G. Warnecke, A high order positivity preserving dg method for coagulation-fragmentation equations, *SIAM Journal on Scientific Computing* 41 (3) (2019) B448–B465.
- [17] J. Jang, H. V. Tran, Discrete coagulation-fragmentation equations with multiplicative coagulation kernel and constant fragmentation kernel, *arXiv preprint arXiv:2409.17974* (2024).
- [18] G. Menon, R. L. Pego, The scaling attractor and ultimate dynamics for smoluchowski’s coagulation equations, *Journal of Nonlinear Science* 18 (2008) 143–190.
- [19] B. Perthame, L. Ryzhik, Exponential decay for the fragmentation or cell-division equation, *Journal of Differential equations* 210 (1) (2005) 155–177.
- [20] I. Stewart, E. Meister, A global existence theorem for the general coagulation–fragmentation equation with unbounded kernels, *Mathematical Methods in the Applied Sciences* 11 (5) (1989) 627–648.
- [21] H. V. Tran, T.-S. Van, Coagulation-fragmentation equations with multiplicative coagulation kernel and constant fragmentation kernel, *Communications on Pure and Applied Mathematics* 75 (6) (2022) 1292–1331.
- [22] C. Connaughton, Numerical solutions of the isotropic 3-wave kinetic equation, *Physica D: Nonlinear Phenomena* 238 (23–24) (2009) 2282–2297.
- [23] C. Connaughton, A. C. Newell, Dynamical scaling and the finite-capacity anomaly in three-wave turbulence, *Physical Review E—Statistical, Nonlinear, and Soft Matter Physics* 81 (3) (2010) 036303.
- [24] C. Connaughton, P. L. Krapivsky, Aggregation–fragmentation processes and decaying three-wave turbulence, *Physical Review E—Statistical, Nonlinear, and Soft Matter Physics* 81 (3) (2010) 035303.
- [25] S. Walton, M.-B. Tran, A numerical scheme for wave turbulence: 3-wave kinetic equations, *SIAM Journal on Scientific Computing* 45 (4) (2023) B467–B492.
- [26] S. Walton, M.-B. Tran, Numerical schemes for 3-wave kinetic equations: A complete treatment of the collision operator, *arXiv preprint arXiv:2402.17481* (2024).
- [27] F. Filbet, P. Laurençot, Numerical simulation of the smoluchowski coagulation equation, *SIAM Journal on Scientific Computing* 25 (6) (2004) 2004–2028.
- [28] N. Bell, V. Grebenev, S. Medvedev, S. Nazarenko, Self-similar evolution of alfvén wave turbulence, *Journal of Physics A: Mathematical and Theoretical* 50 (43) (2017) 435501.
- [29] B. Semisalov, V. Grebenev, S. B. Medvedev, S. Nazarenko, Numerical analysis of a self-similar turbulent flow in bose–einstein condensates, *Communications in Nonlinear Science and Numerical Simulation* 102 (2021) 105903.
- [30] G. Craciun, M.-B. Tran, A reaction network approach to the convergence to equilibrium of quantum boltzmann equations for bose gases, *ESAIM: Control, Optimisation and Calculus of Variations* 27 (2021) 83.
- [31] M. Escobedo, M.-B. Tran, Convergence to equilibrium of a linearized quantum boltzmann equation for bosons at very low temperature, *Kinetic and Related Models* 8 (3) (2015) 493–531.
- [32] I. M. Gamba, L. M. Smith, M.-B. Tran, On the wave turbulence theory for stratified flows in the ocean, *Mathematical Models and Methods in Applied Sciences* 30 (01) (2020) 105–137.

- [33] M.-B. Tran, G. Craciun, L. M. Smith, S. Boldyrev, A reaction network approach to the theory of acoustic wave turbulence, *Journal of Differential Equations* 269 (5) (2020) 4332–4352.
- [34] T. T. Nguyen, M.-B. Tran, On the kinetic equation in zakharov’s wave turbulence theory for capillary waves, *SIAM Journal on Mathematical Analysis* 50 (2) (2018) 2020–2047.
- [35] S. Walton, M.-B. Tran, A. Bensoussan, A deep learning approximation of non-stationary solutions to wave kinetic equations, *Applied Numerical Mathematics* (2022).
- [36] B. Rumpf, A. Soffer, M.-B. Tran, On the wave turbulence theory: ergodicity for the elastic beam wave equation, *arXiv preprint arXiv:2108.13223* (2021).
- [37] E. Cortés, M. Escobedo, On a system of equations for the normal fluid-condensate interaction in a bose gas, *Journal of Functional Analysis* 278 (2) (2020) 108315.
- [38] M. Escobedo, F. Pezzotti, M. Valle, Analytical approach to relaxation dynamics of condensed bose gases, *Annals of Physics* 326 (4) (2011) 808–827.
- [39] M. Escobedo, On the linearized system of equations for the condensate–normal fluid interaction at very low temperature, *Studies in Applied Mathematics* 150 (2) (2023) 448–456.
- [40] M. Escobedo, On the linearized system of equations for the condensate-normal fluid interaction near the critical temperature, *Archive for Rational Mechanics and Analysis* 247 (5) (2023) 92.
- [41] T. T. Nguyen, M.-B. Tran, Uniform in time lower bound for solutions to a quantum boltzmann equation of bosons, *Archive for Rational Mechanics and Analysis* 231 (2019) 63–89.
- [42] A. Soffer, M.-B. Tran, On the dynamics of finite temperature trapped bose gases, *Advances in Mathematics* 325 (2018) 533–607.
- [43] M. Escobedo, J. Velázquez, Finite time blow-up and condensation for the bosonic nordheim equation, *Inventiones mathematicae* 200 (2015) 761–847.
- [44] M. Escobedo, J. Velázquez, On the theory of weak turbulence for the nonlinear Schrödinger equation, Vol. 238, American Mathematical Society, 2015.
- [45] P. Germain, A. D. Ionescu, M.-B. Tran, Optimal local well-posedness theory for the kinetic wave equation, *Journal of Functional Analysis* 279 (4) (2020) 108570.
- [46] C. Collot, H. Dietert, P. Germain, Stability and cascades for the kolmogorov–zakharov spectrum of wave turbulence, *Archive for Rational Mechanics and Analysis* 248 (1) (2024) 7.
- [47] A. Menegaki, l^2 -stability near equilibrium for the 4 waves kinetic equation, *arXiv preprint arXiv:2210.11189* (2022).
- [48] M. Escobedo, A. Menegaki, Instability of singular equilibria of a wave kinetic equation, *arXiv preprint arXiv:2406.05280* (2024).
- [49] P. Germain, J. La, K. Z. Zhang, Local well-posedness for the kinetic mmt model, *arXiv preprint arXiv:2310.11893* (2023).
- [50] M. Dolce, R. Grande, On the convergence rates of discrete solutions to the wave kinetic equation, *arXiv preprint arXiv:2404.14400* (2024).
- [51] G. Staffilani, M.-B. Tran, Condensation and non-condensation times for 4-wave kinetic equations, *arXiv preprint arXiv:2407.18533* (2024).
- [52] G. Staffilani, M.-B. Tran, On the energy transfer towards large values of wavenumbers for solutions of 4-wave kinetic equations, *arXiv preprint arXiv:2407.18508* (2024).
- [53] T. Buckmaster, P. Germain, Z. Hani, J. Shatah, On the kinetic wave turbulence description for nls, *Quarterly of Applied Mathematics* 78 (2) (2020).
- [54] T. Buckmaster, P. Germain, Z. Hani, J. Shatah, Onset of the wave turbulence description of the longtime behavior of the nonlinear schrödinger equation, *Inventiones mathematicae* 225 (2021) 787–855.

- [55] C. Collot, P. Germain, Derivation of the homogeneous kinetic wave equation: longer time scales, arXiv preprint arXiv:2007.03508 (2020).
- [56] C. Collot, P. Germain, On the derivation of the homogeneous kinetic wave equation, Communications on Pure and Applied Mathematics (2019).
- [57] Y. Deng, Z. Hani, On the derivation of the wave kinetic equation for nls, in: Forum of Mathematics, Pi, Vol. 9, Cambridge University Press, 2021, p. e6.
- [58] Y. Deng, Z. Hani, Derivation of the wave kinetic equation: full range of scaling laws, arXiv preprint arXiv:2301.07063 (2023).
- [59] Y. Deng, Z. Hani, Long time justification of wave turbulence theory, arXiv preprint arXiv:2311.10082 (2023).
- [60] Y. Deng, A. D. Ionescu, F. Pusateri, On the wave turbulence theory of 2d gravity waves, i: deterministic energy estimates, Communications on Pure and Applied Mathematics (2022).
- [61] A. Dymov, S. Kuksin, Formal expansions in stochastic model for wave turbulence 1: kinetic limit, Communications in Mathematical Physics 382 (2021) 951–1014.
- [62] A. Dymov, S. Kuksin, Formal expansions in stochastic model for wave turbulence 2: method of diagram decomposition, Journal of Statistical Physics 190 (1) (2023) 3.
- [63] A. V. Dymov, S. B. Kuksin, On the zakharov–l’vov stochastic model for wave turbulence, in: Doklady Mathematics, Vol. 101, Springer, 2020, pp. 102–109.
- [64] A. Dymov, S. Kuksin, A. Maiocchi, S. Vlăduț, The large-period limit for equations of discrete turbulence, in: Annales Henri Poincaré, Vol. 24, Springer, 2023, pp. 3685–3739.
- [65] P. Germain, H. Zhu, On universality for the kinetic wave equation, arXiv preprint arXiv:2402.14773 (2024).
- [66] R. Grande, Z. Hani, Rigorous derivation of damped-driven wave turbulence theory, arXiv preprint arXiv:2407.10711 (2024).
- [67] Z. Hani, J. Shatah, H. Zhu, Inhomogeneous turbulence for wick nls, arXiv preprint arXiv:2309.12037 (2023).
- [68] A. Hannani, M. Rosenzweig, G. Staffilani, M.-B. Tran, On the wave turbulence theory for a stochastic kdv type equation—generalization for the inhomogeneous kinetic limit, arXiv preprint arXiv:2210.17445 (2022).
- [69] J. Lukkarinen, H. Spohn, Weakly nonlinear schrödinger equation with random initial data, Inventiones mathematicae 183 (2011) 79–188.
- [70] X. Ma, Almost sharp wave kinetic theory of multidimensional kdv type equations with $d \geq 3$, arXiv preprint arXiv:2204.06148 (2022).
- [71] G. Staffilani, M.-B. Tran, On the wave turbulence theory for a stochastic kdv type equation, arXiv preprint arXiv:2106.09819 (2021).
- [72] W. Hundsdorfer, J. G. Verwer, Numerical solution of time-dependent advection-diffusion-reaction equations, Vol. 33, Springer Science & Business Media, 2013.
- [73] P. Linz, Convergence of a discretization method for integro-differential equations, Numerische Mathematik 25 (1975) 103–107.
- [74] A. Soffer, M.-B. Tran, On the energy cascade of 3-wave kinetic equations: beyond kolmogorov–zakharov solutions, Communications in Mathematical Physics 376 (3) (2020) 2229–2276.

(Arijit Das) DEPARTMENT OF MATHEMATICS, CHAIR FOR DYNAMICS, CONTROL, MACHINE LEARNING AND NUMERICS (ALEXANDER VON HUMBOLDT PROFESSORSHIP), FRIEDRICH-ALEXANDER UNIVERSITY ERLANGEN-NUREMBERG, ERLANGEN, GERMANY.

Email address, Arijit Das: `arijit.das@fau.de`

(Minh-Binh Tran) DEPARTMENT OF MATHEMATICS, TEXAS A&M UNIVERSITY, COLLEGE STATION, TX, 77843 USA

Email address, Minh-Binh Tran: `minhbinh@tamu.edu`